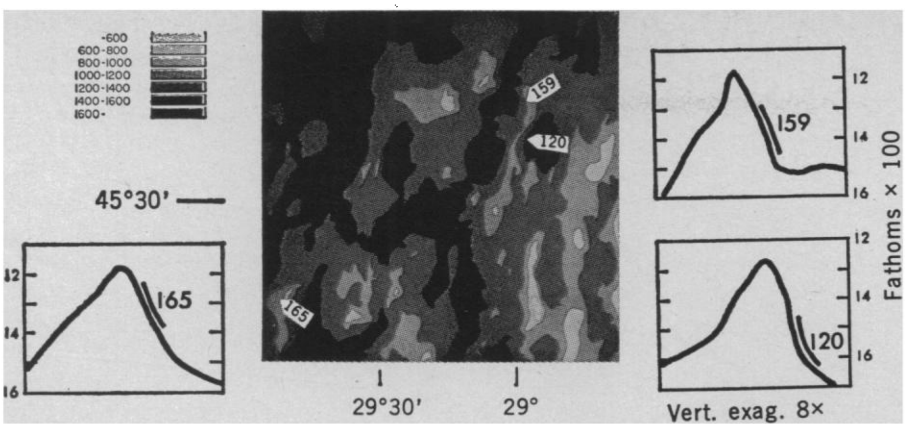

Fig. 1. Simplified bathymetric chart of the western High Fractured Plateau at 45°N, contoured at 200-fathom (365.6-m) intervals, showing station locations and vertical profiles of the dredging operations.

envelop relict cores of pyroxene and olivine. Biotite is only of secondary importance, but occurs in higher concentrations within the tear-shaped xenoliths, where it is associated with pale green hornblende differing in optical characteristics from the large crystals in the host rocks. Accessory minerals include magnetite, chrome spinel, apatite, sphene, and allanite.

Specimen AG-159-35 represents one of the more melanocratic rocks containing numerous basic xenoliths, whereas AG-159-39 is one of the more leucocratic, xenolith-free specimens (Tables 2 and 3). Both diorite analyses show unusually high ratios of soda to potash, which, together with the albite borders on some of the plagioclases, are reminiscent of the albitized diorities characteristic of alpine ultramafic intrusive complexes (*7*). Thus, the more melanocratic specimens are similar to the quartz-diorites of the alpine ultramafic association, and the leucocratic specimens are similar to trondhjemites of these environments.

The ferromanganese coating on the diorites is about 5 mm thick, less than that on the associated serpentinites and basalts (up to 15 mm); from previous calibration of the rate of ferromanganese deposition in the area (*5*) one can estimate that the diorites were first exposed to the ocean water some 3 million years ago (well before the Pleistocene ice ages), probably at the time of the final upthrusting of the seamount blocks. Relatively recent vertical movements of the oceanic crust may therefore have taken place in these areas of the High Fractured Plateau quite remote from the axis of the ridge. Basalts in the vicinity of the major diorite occurrences have been dated by whole rock K-Ar and by fission-track techniques to be from 8 to 12 million years old (*5*). Two K-Ar dates on the hornblendes from the diorites gave an average age of 9 ± 1.3 million years (*6*). In addition, oxygen isotopic compositions (*6*) place the diorites within the range obtained for the associated basalts and serpentinites.

The concordant ages and isotopic compositions and the chemistry and physical appearance of the diorites are strong indication that they occur *in situ* on the faulted scarps of the seamounts sampled, and that they are directly related to the basalt, metabasalt, serpentinized gabbro, and peridotite association found in the area at 45°N. Their *in situ* occurrence on these seamounts is proof that magmatic differentiation has progressed farther than is generally thought possible in mid-oceanic ridge environments. It also suggests that strong similarities may exist between the oceanic ridges and the synorogenic igneous complexes of the Alpine or Ophiolitic type. Forty-five dredge stations were established in a relatively small area (150 by 250 km) before these diorites were detected. They are obviously not common mid-oceanic rock types, but neither are they abundant in alpine complexes; however, since they do occur, it is possible that other magmatic derivatives may also have been collected in the past, but were promptly discarded as ice-rafted erratics (*2*, *6*).

F. Aumento

Geological Survey of Canada, Ottawa, Ontario

References and Notes

1. J. R. Cann, and B. M. Funnel, *Nature* **213**, 661 (1967); J. R. Conolly and M. Ewing, *ibid.* **208**, 135 (1965); M. Ewing, *Nat. Geol. Mag.* **96**, 611 (1949); B. C. Heezen, *Geol. Soc. Amer. Spec. Pap.* **65**, 99 (1959); J. Murray and A. F. Renard, *H.M.S. Challenger Report* (1891), p. 322; R. M. Pratt, *Deep-Sea Res.* **8**, 162 (1961); S. H. Quon and E. G. Ehlers, *Bull. Geol. Soc. Amer.* **74**, 1 (1963).
2. F. Aumento and B. D. Loncarevic, *Can. J. Earth Sci.* **6**, 11 (1969).
3. R. K. Wanless, R. D. Stevens, G. R. LaChance, C. M. Edmonds, *Can. Geol. Surv. Pap.* **67-2**, Part A (1967).
4. F. Aumento, *Science* **161**, 1338 (1968).
5. F. Aumento, *Trans. Amer. Geophys. Union*, **50**, 352 (1969).

6. I thank K. Muehlenbachs, M. J. Keen, A. Hayatsu, and A. G. Plant for oxygen isotopic data, sedimentary thickness measurements, radiometric dating, and electron-probe analyses, respectively.

7. T. P. Thayer, and G. R. Himmelberg, *Int. Geol. Congr. 22nd* **1**, 175 (1968).

22 April 1969; revised 22 May 1969

Hydrothermal Ore Deposits in the Western United States: A New Concept of Structural Control of Distribution

Abstract. *Empirical plotting of four sets of equidistantly spaced shear stress trajectories, based on regularities in distribution of actual faults and ore veins in the continental area and on the landward prolongation of the big fracture zones of the northeastern Pacific, gives rise to a prospecting net for the western United States. Preferential accumulation of big ore deposits (including such deposits as Bingham and Tintic) along landward prolongation of the main fracture zones of northeastern Pacific, in the vicinity of intersections of four systems of trajectories, and along boundaries of crustal blocks suggests several possibilities for prospecting for unknown hydrothermal deposits in the Cordilleran part of the United States.*

The method of constructing empirical prospecting nets, which I described previously (*1*, *2*) has been put to practical application in the silver, lead, and zinc Pribram ore field, Czechoslovakia (*3*). The existence of a north-northwest set of faults empirically derived for a part of Scotland (and previously not known in geological maps of that area), as a complementary set to the well-known northeast-trending wrench-faults of the "Great Glen" strike, was ascertained by a recent geophysical survey (*4*). The Tyndrum district lies exactly at one of the intersections of these faults [Fig. 7 in (*2*)].

In the present report I attempt to apply the same method to the study of regularity in the distribution of hydrothermal ore deposits and to construct an empirical prospecting net for the Cordilleran part of the United States.

If we depict, at least semiquantitatively, the concentration of metals in hydrothermal deposits of the United States and the adjacent part of Canada (Fig. 1), we may observe that, especially in the western Cordilleran area, the most important hydrothermal deposits are concentrated essentially into three groups or west-east trending belts. One of these belts roughly follows the landward prolongation of two big fracture zones of the northeastern Pacific floor—Mendocino and Pioneer (marked by dotted lines), which were described by Menard (*5*). The comparable distances D_1 and D_2 between the landward prolongation of Mendocino and the important groups of deposits located north and south of it suggest that their position may also be controlled by similar east-west trending tectonic lines.

The position of the big deposits of Sudbury, Blind River, Procupine-Kirkland Lake-Noranda, and Lake Superior in the eastern part of the continent, corresponds surprisingly to the latitude position of the big hydrothermal ore deposits in the western part of the United States and Canada (Butte, Coeur d'Alene, and Sullivan) which suggests that the ascent of ore fluids might have been controlled by upward propagating of major faults of deeper portions of the earth's crust across the whole territory of North America. One of these hypothetical directions was plotted as an empirical east-west trending trajectory going across Butte and Sudbury.

Figure 2, giving in greater detail the distribuiton of hydrothermal ore deposits specifically in the Cordilleran part of the United States, shows that they are not equally distributed and have a tendency to group in knots and elongated belts. Even on this more detailed scale, a relation of the ore deposits to the landward prolongation of the big fracture zones of the northeastern Pacific floor, namely, to the Mendocino fracture zone, is apparent.

Several geological criteria in favor of the continuation of Mendocino through or below North America have been presented by Gilliland (*6*). Fuller (*7*) found comparable interruptions in magnetic anomalies near 40°N at sev-

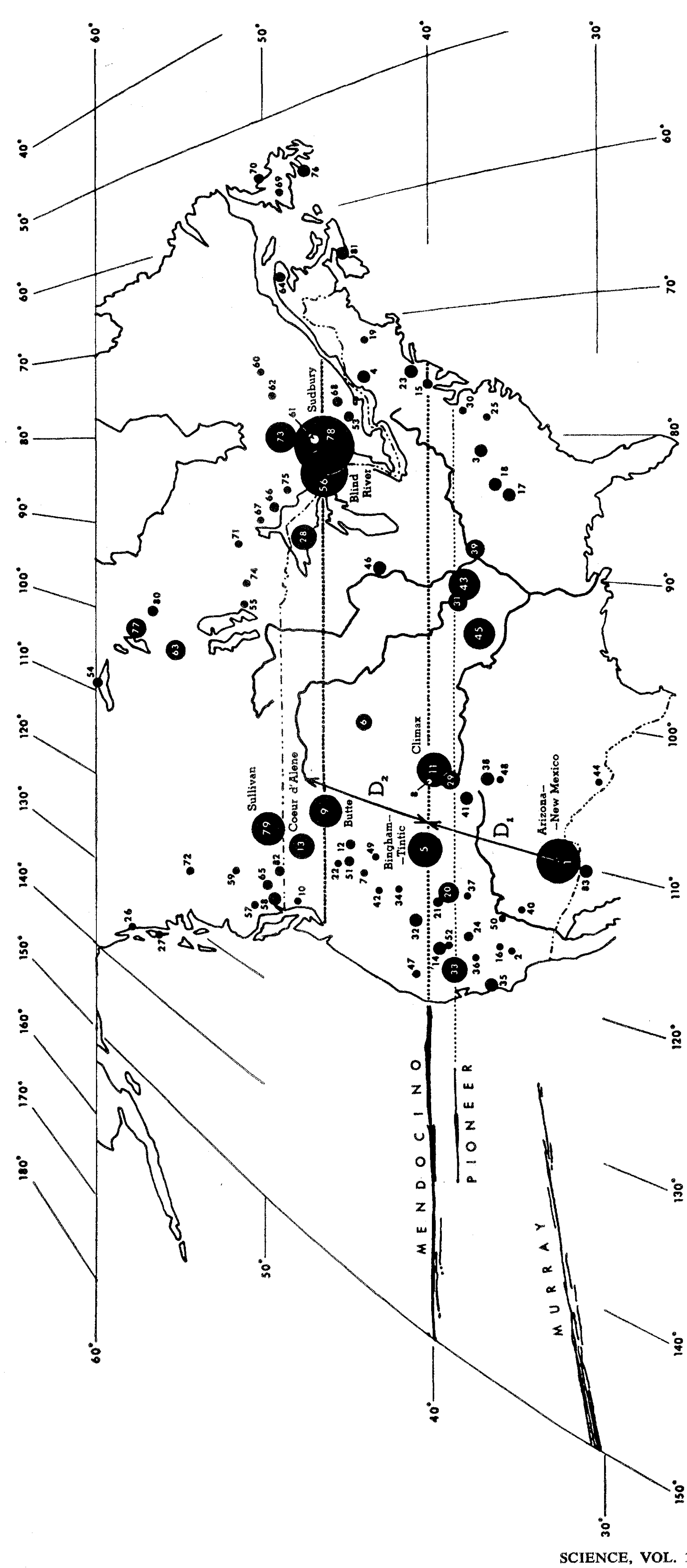

eral places in the United States (as far east as Indiana), which suggests landward prolongation of Mendocino. The above data justify my using the strike of the big east-west fracture zones in defining the direction of one set of shear stress trajectories in the western United States.

Four sets of trajectories are distinguished (Fig. 3).

1) *The east-west set of shear stress trajectories.* The straight course of the Mendocino Fault was taken as the direction of trajectories in the east-west set, and the distance between Mendocino and Pioneer as the unit interval (Fig. 3). The spacing between Mendocino and Murray is comparable to the spacings between the other main fracture zones of the Pacific floor off the west coast of the North and South American continents: Mendocino, Murray, Molokai, Clarion, Clipperton, Galapagos, and Marquesas [see Fig. 3.1. in (*8*)].

Along the 0-trajectory (Mendocino trajectory) there are pronounced accumulations of deposits, especially in two areas. One of them is in Utah, including the well-known deposits of Bingham and Tintic, and the other in Colorado, which represents the beginning of a southwest-trending belt of mineralization. The apparent relation of east-west striking faults in the area of the Uinta Uplift to the 0-trajectory is clearly shown in the tectonic map of the United States (*9*).

If we plot spacings equal to three and four unit intervals northward from Mendocino, we reach trajectories +3 and + 4. The continental prolongation of trajectory + 3 is strikingly followed by the Columbia River, and along it is localized a very important knot of Montana ore deposits (including Butte). Similarly, at trajectory + 4 a great accumulation of ore metals took place (Coeur d'Alene). For another one or one and a half unit intervals northward, we have the world's biggest zinc deposit of Sullivan in Canada.

If this accumulation of big ore deposits along the group of three trajectories (+ 3, + 4, and + 5) had been conditioned by an upward propagation of a hitherto unknown east-west trending fracture zone of deeper portions of the earth's crust, having structural importance similar to that of the landward prolongation of Mendocino and Pioneer (trajectories 0 and − 1), then it would be likely to suppose that the

Fig. 1. Concentration of the most important hydrothermal ore deposits of the United States and the adjacent part of Canada into three groups or west-east trending belts, one of which roughly follows the landward prolongation of two big fracture zones of the northeastern Pacific floor—Mendocino and Pioneer (marked by dotted lines). The comparable distances D_1 and D_2 between the landward prolongation of Mendocino and the important groups of deposits located north and south of it suggest that their position may also be controlled by similar west-east trending tectonic lines. The distribution and expression of the magnitude of ore deposits was adopted from Laffitte and Rouveyrol (*20*) with omission of unquestionably sedimentary, chromite, and placer deposits. Ore deposits of controversial origin (mainly the Mississippi Valley type deposits and the Blind River uranium deposit) were retained. The course of the fracture zones of the northeastern Pacific was taken over from Menard (*8*). The diameter of the circles on the map is related to the tonnage of the respective metals in the deposits and is different for different metals. The metals used by Laffitte and Rouveyrol (*20*) to categorize each deposit are given in parentheses; if in a category (Pb+Zn+Ag) only one of the metals is important for a given deposit, its symbol is underlined. The magnitude of the deposits is used here only in a semiquantitative way.

United States

1 - Arizona–New Mexico (Cu, Mo, Pb+Zn+Ag)
2 - Atolia, California (W)
3 - Austinville, Gossan Lead, Virginia (Pb+Zn+Ag, Cu)
4 - Balmat, New York (Pb+Zn+Ag)
5 - Bingham and Tintic, Utah (Cu, Mo, Au, Pb+Zn+Ag)
6 - Black Hills, South Dakota (Au)
7 - Boise, Idaho (Au)
8 - Boulder, Colorado (W)
9 - Butte, Montana (Cu, Pb+Zn+Ag, Au)
10 - Chelan, Washington (Au, Cu)
11 - Climax, Colorado (Mo, W)
12 - Cobalt, Idaho (Co)
13 - Coeur d'Alene, Idaho (Pb+Zn+Ag)
14 - Comstock Lode, Nevada (Au, Pb+Zn+Ag)
15 - Cornwall, Pennsylvania (Co, Cu)
16 - Darwin, California (Pb+Zn+Ag)
17 - Ducktown, Tennessee (Cu)
18 - East Tennessee (Pb+Zn+Ag)
19 - Elisabeth, Vermont (Cu)
20 - Ely, Nevada (Au, Cu)
21 - Eureka, Nevada (Au, Pb+Zn+Ag)
22 - French Creek, Idaho (Au)
23 - Franklin, New Jersey (Pb+Zn+Ag)
24 - Goldfield–Tonopah, Nevada (Au, Pb+Zn+Ag)
25 - Hamme, North Carolina (W)
26 - Juneau, Alaska (Au)
27 - Ketchikan, Alaska (Mo)
28 - Lake Superior, Michigan (Cu)
29 - Leadville and Cripple Creek, Colorado (Pb+Zn+Ag, Au)
30 - Louisa, Virginia (Cu)
31 - Magnet Cove, Arkansas (Ba)
32 - Mill City (Golconda), Nevada (W)
33 - Mother Lode, Middle California (Au)
34 - Mountain City, Nevada (Cu)
35 - New Almaden and New Idria, California (Hg)
36 - Pine Creek, California (W)
37 - Pioche, Nevada (Pb+Zn+Ag)
38 - Questa, New Mexico (Mo)
39 - Rosiclare, Illinois (F)
40 - San Francisco, Arizona (Au)
41 - San Juan, Telluride, Colorado (Au, Pb+Zn+Ag)
42 - Silver City, Idaho (Au)
43 - Southeast Missouri (Pb+Zn+Ag)
44 - Terlingua, Texas (Hg)
45 - Tristate, Missouri–Kansas–Oklahoma (Pb+Zn+Ag)
46 - Upper Mississippi, Wisconsin–Illinois (Pb+Zn+Ag)
47 - West Shasta, California (Cu)
48 - Willow Creek, New Mexico (Pb+Zn+Ag)
49 - Wood River, Idaho (Pb+Zn+Ag)
50 - Yellow Pine, Nevada (Pb+Zn+Ag)
51 - Yellow Pine, Idaho (Au, W)
52 - Yerington, Nevada (Cu)

Canada

53 - Bancroft, Ontario (U)
54 - Beaverlodge, Saskatchewan (U)
55 - Bisset, Manitoba (Au)
56 - Blind River, Algoma District, Ontario (U)
57 - Bralorne, British Columbia (Au)
58 - Britannia, British Columbia (Au, Cu)
59 - Cariboo, British Columbia (Au)
60 - Chibougamau, Quebec (Au, Cu)
61 - Cobalt, Ontario (Co)
62 - Coniagas Mines, Quebec (Pb+Zn+Ag)
63 - Flin Flon, Manitoba (Cu, Pb+Zn+Ag, Au)
64 - Gaspe, Quebec (Cu)
65 - Giant Nickel, British Columbia (Cu, Ni)
66 - Geco Mines, Ontario (Cu, Pb+Zn+Ag)
67 - Little Longlac, Ontario (Au)
68 - New Calumet, Quebec (Pb+Zn+Ag)
69 - Newfoundland (Cu, Au)
70 - Newfoundland (Cu, Pb)
71 - Pickle Crow, Ontario (Au)
72 - Pinchi Lake, British Columbia (Hg)
73 - Porcupine and Kirkland Lake (Ontario) and Noranda (Quebec) (Au, Cu, Pb+Zn+Ag)
74 - Red Lake, Ontario (Au)
75 - Renabie, Ontario (Au)
76 - Saint Lawrence, Newfoundland (F)
77 - Sheritt Gordon, Manitoba (Co, Cu, Ni)
78 - Sudbury, Ontario (Ni, Co, Cu, Pt)
79 - Sullivan, British Columbia (Pb+Zn+Ag)
80 - Thompson, Manitoba (Ni)
81 - Walton, Nova Scotia (Ba)
82 - (Au, Cu)

Mexico

83 - Cananeá, Sonora (Cu, Mo)

big concentration of ore deposits in Arizona may have been conditioned by a similar landward prolongation of the Murray fracture zone and accompanying effects along the nearest north- and south-lying trajectories. Anyway, it seems evident that all trajectories of the east-west set are not of the same structural importance.

2) *The north-south set of shear stress trajectories.* There are many north-south trending faults in the broad area of the western United States. A great part of the Rocky Mountains follows this trend; certainly one of the most important shear stress trajectories of the north-south set must be located along the course of this mountain chain (trajectory +9). Another trajectory of this set has been tentatively plotted along the southern part of the Colorado River which, as a whole, has a pronounced north-south trend before it abruptly changes its course to the east. While constructing the north-south set of shear stress trajectories, the general tendency of the Rocky Mountains and many of the north-south trending faults to curve convexly to the east was respected.

In the vicinity of intersection of the Rocky Mountains +9 trajectory with the Mendocino trajectory there is an accumulation of ore deposits. Another important ore knot, in Utah, lying along the Mendocino trajectory (near the Great Salt Lake) is located around the intersection with the north-south tectonic boundary of the Wasatch Fault Block, in the southern prolongation of which the long Sevier Fault runs. Thus, one of the shear stress trajectories (+6) was plotted along this direction. The distance between the trajectory plotted along the southern part of the Colorado River (trajectory +5) and the one plotted through the group of deposits in Utah (trajectory +6) was chosen as a unit interval in the north-south set of trajectories. The distance between the important ore knots in Utah and Colorado is equal to three unit intervals. The distance between the +9 Rocky Mountains trajectory and the +5 trajectory, which is for a long distance followed by the Colorado River and in the vicinity of which the Coeur d'Alene District lies, is equal to four unit intervals. Thus, it seems that even in the north-south set of shear stress trajectories there appear broad zones of structurally greater importance manifesting themselves along more than one neighboring trajectory (in this case along trajectories +5 and +6).

Three ore knots are present along the +6 trajectory of the north-south set and are located by the intersection of the +6 trajectory with three important trajectories of the east-west set—the +3 Columbia trajectory, Mendocino trajectory, and one of the trajectories whose structural importance may be influenced by the landward prolongation of the Murray fracture zone (trajectory −3) (see the ore knots encircled on the north-south trajectory +6 in Fig. 3).

Of the rivers that show a relation to the north-south set of trajectories, in addition to the Colorado River, the Green River especially follows one of them (the +7 trajectory) quite pronouncedly.

3) *The northeast set of shear stress trajectories.* The direction of the northeast set of trajectories was chosen to run exactly through the northeast and southwest corners of the fields bounded by the east-west and north-south trajectories. The northeast trajectories also show a pronounced equidistant distribution of several ore knots or other kind of concentration of ore deposits, especially along the equidistantly spaced trajectories A_{-3} (Butte and others in Montana), A_{-6} (Bingham and Tintic and others in Utah), A_{-9} (the long belt of Colorado deposits and some deposits in Arizona), and A_{-12} (a group of deposits in southwestern New Mexico and the southeastern part of Arizona).

Importance of the northeast fractures for localization of hydrothermal ores of this broad area was statistically studied by Landwehr (*10*), so that many fractures of this trend were proved. The Colorado River, especially in its northeastern part, follows this trend for a long distance.

Fig. 2. Main hydrothermal ore deposits in the western United States as a basis for discussing the regularities in their distribution in Fig. 3. Plotting of ore deposits substantially after Burnham (*21*), Landwehr (*10*), and Laffitte and Rouveyrol (*20*) with their differentiation into three relative categories. The fracture pattern of the northeastern Pacific floor after Menard's map (*8*), simplified.

Arizona: 1, Ajo; 2, Bagdad; 3, Bisbee; 4, Bradshaw Mountains; 5, Christmas; 6, Congress; 7, Copper Basin; 8, Esperanza; 9, Globe–Miami; 10, Iron King; 11, Jerome; 12, Johnson; 13, Katherine; 14, Kofa; 15, Mammoth; 16, Mission; 17, Morenci; 18, Oatman, San Francisco; 19, Patagonia; 20, Pima; 21, Ray; 22, Rich Hill; 23, San Manuel; 24, Silver Bell; 25, Superior; 26, Swansea; 27, Tombstone; 28, Turquoise; and 29, Vulture.

California: 1, Alleghany; 2, Angels–Carson; 3, Atolia; 4, Bagdad–Chase; 5, Bodie; 6, Calico; 7, Cerro Gorde; 8, Darwin; 9, Foothill; 10, Grass Valley; 11, Julian; 12, Mojave; 13, New Almaden; 14, New Idria; 15, Pine Creek, Bishop District; 16, Plumas County; 17, Plymouth–Jackson; 18, Randsburg; 19, Shasta County; and 20, Wildrose.

Colorado: 1, Alma; 2, Aspen; 3, Bonanza; 4, Breckenridge; 5, Central City; 6, Climax; 7, Crested Butte; 8, Creede; 9, Cripple Creek; 10, Georgetown; 11, Gilman; 12, Gold Hill; 13, Jamestown; 14, Lake City; 15, La Plata; 16, Leadville; 17, Monarch; 18, Montezuma; 19, Ouray; 20, Rico; 21, Silver Cliff; 22, Silverton; 23, Summitville; and 24, Telluride.

Idaho: 1, Atlanta; 2, Bayhorse; 3, Blackbird; 4, Boise; 5, Coeur d'Alene (Wallace); Cobalt, see Blackbird; French Creek (not given); 6, Mackay; 7, Pearl Horse, Shoe Bend; 8, Quartsburg; 9, Silver City; 10, South Mountain; Wallace, see Coeur d'Alene; 11, Wood River; 12, Yellow Jacket; and 13, Yellow Pine.

Montana: 1, Argenta; 2, Butte; 3, Elkhorn; 4, Hecla; 5, Helena; 6, Hughesville; 7, Marysville; 8, Neihart; 9, Philipsburg; 10, Rimini; and 11, Virginia City.

Nevada: 1, Aurora; 2, Battle Mountain; 3, Candelaria; 4, Comstock; 5, Cortez; 6, Ely; 7, Eureka; 8, Ferguson; 9, Getchell; 10, Golconda; 11, Goldfield; 12, Hawthorn; 13, Jarbidge; 14, Manhattan; 15, Midas; Mill City, see Golconda; 16, Mountain City; 17, Pioche; 18, Reese River; 19, Rochester; 20, Round Mountain; 21, Silver Peak; 22, Tonopah; 23, Tuscarora; 24, Tybo; 25, Yellow Pine; and 26, Yerington.

New Mexico: 1, Elisabethtown; 2, Hillsboro; 3, Lordsburg; 4, Magdalena; 5, Mogollon; 6, Pecos; 7, Questa; 8, San Pedro; 9, Santa Rita, Central Mining District; and, 10, Tyrone; Willow Creek (not given).

Oregon: 1, Blue Mountains.

South Dakota: 1, Black Hills.

Utah: 1, Bingham; 2, Cottonwood; 3, Drum Mountains; 4, Fish Springs; 5, Gold Hill; 6, Mercur; 7, Ophir; 8, Park City; 9, San Francisco; 10, Stockton; and 11, Tintic.

Washington: 1, Chelan; 2, Metaline; and 3, Republic.

4) *The northwest set of shear stress trajectories.* The direction of the northwest set of trajectories was also chosen to run through two opposite corners of the fields originated by transection of the east-west and north-south set of trajectories. The northwest trajectories plotted in this way show an excellent agreement with the strike of the faults of the San Andreas system in California. Also in this set of trajectories, equidistant distribution of several ore knots becomes apparent: A group of Arizona ore deposits is located along the B_3 trajectory and the important knot in Utah occurs along B_6. Along the B_9 trajectory are found the Coeur d'Alene District in Idaho and the group of Montana deposits including Butte; the trajectory marks the northeastern end of the Colorado ore belt.

Distribution of hydrothermal ore deposits in the western United States shows a relation to all of the four systems of empirical equidistantly spaced shear stress trajectories (Fig. 3). Some of the important ore knots lie along the continental prolongation of big fracture zones of the eastern Pacific. In the northeast and northwest set of trajectories, every third trajectory is structurally more important than the other two.

In Fig. 3, such a plotting of multiples of three unit intervals in the northeast and northwest sets of trajectories has given rise to a net of big blocks bounded by expected big northeast- and northwest-trending deep faults. Not all of the corners of these fields (horizontal projection of big blocks) are of equal structural importance. For instance, the block bounded by the northwest trajectories B_6 and B_9 and by the northeast trajectories A_{-6} and A_{-9} has two corners in which trajectories of all the four systems intersect, while the other two corners show intersections of two trajectories of this order only. In the vicinity of corners with intersections of four trajectories, there are important ore body accumulations in Utah (near the Great Salt Lake) and in Colorado. In the neighborhood of the other two

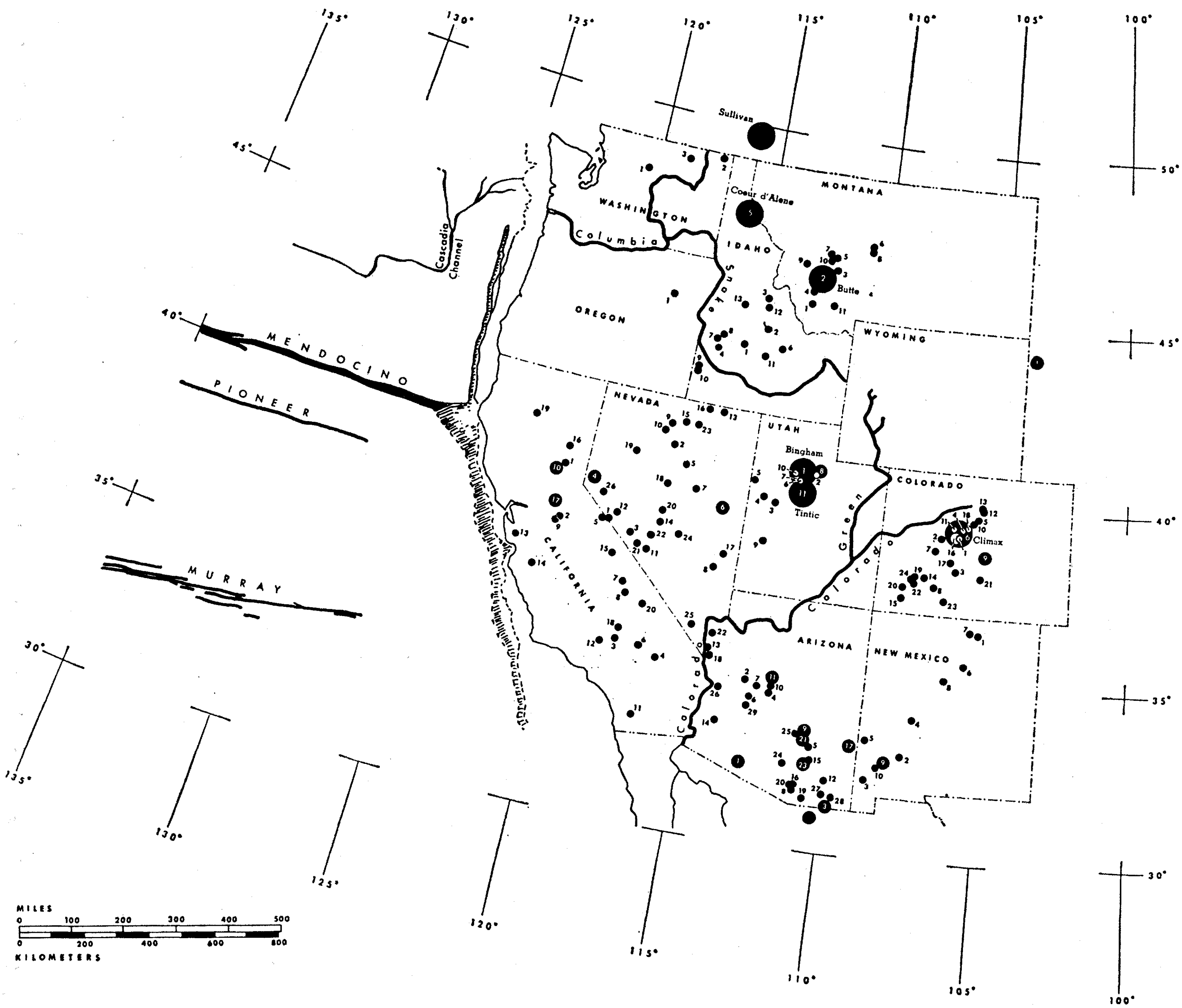

corners, where only two trajectories intersect, none of the deposits plotted in Figs. 2 and 3 are located. Similar relations may be observed in two other big blocks: In the block bounded by the B_6 and B_9 trajectories of the northwest set and by the trajectories A_{-3} and A_{-6} of the northeast set, the corners with intersections of four trajectories are occupied by an important group of Montana deposits, including Butte, and by the Utah deposits near the Great Salt Lake, including Bingham and Tintic. In the vicinity of the other two corners, where only two trajectories intersect, none of the deposits of Figs. 2 and 3 are located. Not so pronounced, but nevertheless rather similar, relations may be observed in the block bounded by the B_3 and B_6 trajectories of the northwest set and the A_{-6} and A_{-9} trajectories of the northeast set.

Besides preferential accumulation of ore deposits around structurally more important corners of the above big blocks, a tendency of these deposits to concentrate along the "boundary faults" seems apparent. For instance, the pronounced belt of Colorado de-

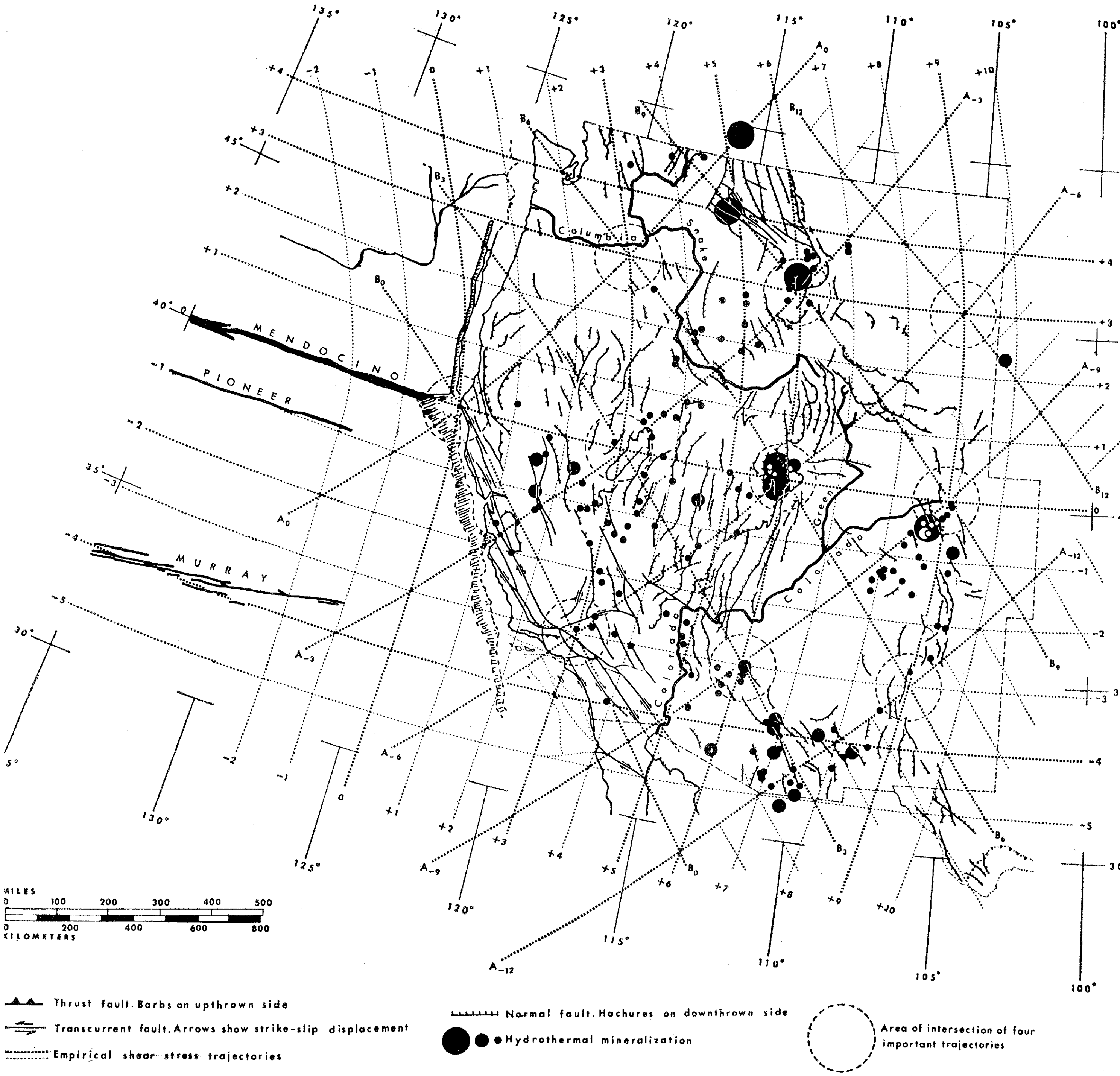

Fig. 3. Empirical prospecting net for hydrothermal ore deposits in the western United States. Tendency toward preferential concentration of ore deposits (i) along landward prolongation of the big fracture zones of the northeastern Pacific, (ii) in the vicinity of the intersection of four trajectories, and (iii) along boundaries of big blocks bounded by the northeast- and northwest-trending shear stress trajectories. The distribution of faults in the continental area are after King (*22*), and the fracture pattern of the northeastern Pacific floor is simplified from Menard's map (*8*).

posits roughly follows the boundary of two adjacent big blocks, being substantially located along the trajectory A_{-9} of the northeast set. Similarly, several ore deposits of New Mexico and of southeastern Arizona seem to be emplaced along A_{-12} trajectory of the northeast set and the B_3 trajectory of the northwest set, that is, along two of the trajectories bounding another big block at its southern side. The corner, where the above B_3 and A_{-12} trajectories intersect, does not, unlike the preceding ones, represent an intersection of four trajectories, but only two.

The regularities as described above generally fit well in nearly the whole area of the western United States, with the exception of the westernmost part (mainly California).

Preliminary comparison of the prospecting net with the Bouger anomaly map of the United States (*11*) shows a relation in each set of trajectories. Considering the north-south set, trajectories $+6$ and $+9$ show the most pronounced relation to the gravity anomaly pattern. This relation of ore deposits to the system of four sets of empirical shear stress trajectories applies to hydrothermal deposits of various ages. The deep faults to which the trajectories are believed to correspond served interruptedly as supply channels in the metallogenetic history of this large region.

Structural control of ore deposition in the Cordilleran part of the United States has been the subject of study for many years [compare especially Butler (*12*) and other papers of the "Lindgren Volume," and many papers in the recent "Graton-Sales Volume" edited by Ridge (*13*)]. The unequal distribution of hydrothermal ore deposits of the western United States was underlined, for example, by Billingsley and Locke (*14*), who dealt with structure of the individual ore districts. Mayo (*15*) recognized the role of four systems of faults and their intersections on the localization of several bodies of igneous rocks and ore deposits in the area. Badgley (*16*) recognized that the deposits of Bingham, Park City, Tintic, and Cripple Creek lie close to the landward projection of the Mendocino zone. A relation of the Bingham District to the prolongation of the Mendocino zone was also suggested by Wisser (*17*). Landwehr (*10*) defined seven northeast-trending belts of major mineralization in this area and expressed the opinion that these belts reflect zones of deep rupture in the earth's crust.

Structural patterns of some ore districts or of larger areas of the western United States, as expressed by some authors, show a promising relation to the net of shear stress trajectories of Fig. 3. An example is the structural pattern of the southwestern copper region given by Badgley [see Fig. 5 in (*18*)].

In the central United States Heyl (*19*) recognized that economically promising sulfide deposits occur along a west-trending fault system crossing Kentucky and Missouri near the 38th parallel, particularly at associated cryptoexplosion structures along it and at the intersection of the fault system with the Cincinnati arch. Thus, it seems that the importance of the east-west shear stress trajectories for prospecting need not be limited only to the area of the western United States.

JAN KUTINA
Department of Geological Sciences, Lehigh University, Bethlehem, Pennsylvania 18015

References and Notes

1. J. Kutina, J. Pokorný, M. Veselá, *Econ. Geol.* **62**, 390 (1967); correction, *ibid.*, p. 1010.
2. J. Kutina, in *Endogenous Ore Deposits* (Proceedings of Section 7, 23rd International Geological Congress, Prague, 1968), pp. 99–110.
3. J. Kutina and A. Telupil, *Vestn. Ústredniho Ústavu Geol.* **41**, 431 (1966).
4. A. C. McLean and S. Johnstone, personal communication.
5. H. W. Menard, *Bull. Geol. Soc. Amer.* **66**, 1149 (1955).
6. W. N. Gilliland, *Science* **137**, 685 (1962).
7. M. D. Fuller, *Geophysics* **29**, 602 (1964).
8. H. W. Menard, *Marine Geology of the Pacific* (McGraw-Hill, New York, 1964).
9. G. V. Cohee *et al.*, *Tectonic Map of the United States, 1 : 2,500,000* (U.S. Geological Survey and American Association of Petroleum Geologists, Washington, D.C., 1962).
10. W. R. Landwehr, *Econ. Geol.* **62**, 494 (1967).
11. G. P. Woolard and H. R. Joesting, Eds., *Bouger Gravity Anomaly Map of the United States, 1 : 2,500.000* (American Geophysical Union and U.S. Geological Survey, Washington, D.C., 1964).
12. B. S. Butler, in *Ore Deposits of the Western States* (Lindgren Volume), J. W. Finch *et al.*, Eds. (American Institute of Mining, Metallurgical, and Petroleum Engineers, New York, 1933), pp. 198–326.
13. J. D. Ridge, Ed., *Ore Deposits of the United States, 1933—1967* (Graton-Sales Volume) (American Institute of Mining, Metallurgical, and Petroleum Engineers, New York, 1968), vols. 1 and 2.
14. P. Billingsley and A. Locke, *Trans. AIME* **144**, 9 (1941).
15. E. B. Mayo, *Mining Engng.* **10**, pt. 3, 1169 (1958).
16. P. C. Badgley, "Tectonic analysis as an exploration tool," *Soc. Mining Eng., AIME,* preprint 59, 169 [from S. F. Kelly, *Western Miner and Oil Rev.* (Oct. 1960)].
17. E. H. Wisser, *Can. Mining Metal. Bull.* **52**, 34 (1959).
18. P. C. Badgley, *Trans. AIME* **223**, 381 (1962).
19. A. V. Heyl, *Econ. Geol.* **63**, 585 (1968).
20. P. Laffitte and P. Rouveyrol, *Carte Minière du Globe sur Fond Tectonique au 20,000,000e* (Bureau de Recherches Geologiques et Minière, Paris, 1964).
21. W. Burnham, "Metallogenic Provinces of the Southwestern United States and Northern Mexico" (New Mexico Institute of Mining and Technology, Socorro, Bulletin 65, 1959), pp. 1–76.
22. P. B. King, "Tectonic features," *Tectonic Map of the United States in the Scale 1 : 7,500.000* (U.S. Geological Survey, Washington, D.C., 1967).
23. I thank Dr. J. D. Ryan, chairman of the Department of Geological Sciences, for the support he has given me while I was elaborating this report during my stay at Lehigh University. Dr. Gunnar Kullerud, Geophysical Laboratory, Washington, D.C., offered valuable suggestions that improved the report. I also thank my colleagues in the Department of Geological Sciences for recommending some of the literature references, and I am especially grateful to Charles B. While for constructive discussions.

27 March 1969

Hydrocalcite ($CaCO_3 \cdot H_2O$) and Nesquehonite ($MgCO_3 \cdot 3H_2O$) in Carbonate Scales

Abstract. *Hydrocalcite ($CaCO_3 \cdot H_2O$) with exactly one molecule of hydrate water is the main component of carbonate scales deposited from cold water in contact with air. When the magnesium content of the water is high, the hydrocalcite occurs together with $MgCO_3 \cdot 3H_2O$ (nesquehonite). From the conditions under which hydrocalcite is transformed into calcite and aragonite, it appears that in some cases aragonite in nature may be formed by way of an intermediary of $CaCO_3 \cdot H_2O$.*

Synthesis of $CaCO_3 \cdot H_2O$ has been accomplished by precipitation at $\pm 0°C$ or in the presence of additives such as polyphosphates, $MgCl_2$, and sugar (*1, 2*). It has hitherto not been observed in nature. The compound $MgCO_3 \cdot 3H_2O$, which has been synthesized (*3*), also occurs as the mineral nesquehonite. Both hydrocarbonates are unstable.

It was thus surprising to find that $CaCO_3 \cdot H_2O$ (hereafter called hydrocalcite) is the main component of carbonate scales (i) in air scrubbers of different air-conditioning plants, and (ii) at the mouths of cold water pipes.